

# CHARACTERIZATION OF UNIVERSAL BEHAVIOR IN QCD DIRAC SPECTRA

J.J.M. VERBAARSCHOT  
*Department of Physics and Astronomy,  
University at Stony Brook,  
Stony Brook, NY 11794, USA*

In this lecture we discuss correlations of the QCD Dirac eigenvalues. We find that below a scale of  $E_c \sim \Lambda/L^2$  they are given by chiral Random Matrix Theory. This follows from analytical arguments based on partially quenched Chiral Perturbation Theory and is substantiated by lattice QCD and instanton liquid simulations.

## 1 INTRODUCTION

The low-energy limit of QCD is characterized by two parameters, the chiral condensate,  $\Sigma$ , and the pion decay constant,  $F$ . The chiral condensate is directly related to the density of the smallest eigenvalues of the Dirac operator by means of the Banks-Casher formula<sup>1</sup>. At finite volume, the pion decay constant determines the quark mass scale below which the QCD partition function is given by the zero momentum component of the chiral Lagrangian<sup>2,3</sup>. Below this scale the Dirac eigenvalues are constraint by Leutwyler-Smilga sum rules<sup>3</sup>. On the other hand, the accumulation of small eigenvalues for broken chiral symmetry requires strong interactions<sup>4</sup>. From the study of complex systems (see Guhr et al.<sup>5</sup> for a comprehensive review) we expect that microscopic correlations of eigenvalues of such disordered system are universal and can be described by the simplest model in its universality class. Such a model is chiral Random Matrix Theory (chRMT). The interpretation is that the classical motion of quarks in Euclidean QCD with an additional artificial time dimension is chaotic.

These ideas can be formulated more precisely in terms of partially quenched Chiral Perturbation Theory<sup>6</sup> (pqChPT), which, in addition to the usual quarks, contains valence quarks and their superpartners<sup>7</sup>. If both the Vafa-Witten theorem<sup>8</sup> and the Goldstone theorem apply to this theory, only one mass term consistent with the chiral symmetries of the partition function can be written down. On the other hand, it can be shown<sup>9</sup> that the zero-momentum sector of pqChPT reproduces identically the chRMT distribution of the smallest eigenvalues up to a scale which is the equivalent of the Thouless energy in the theory of mesoscopic systems<sup>11,5</sup>. In units of the level spacing, this scale is given by  $n_c = F^2 L^2 / \pi$  for a box of length  $L$ . This argument proves the conjecture<sup>10</sup> that the correlations of the smallest QCD Dirac eigenvalues are

given by chRMT. The stability of the RMT correlations under deformations of the ensemble as shown by universality studies<sup>12,13,14,15,16 17,18,19,20</sup> strengthens our confidence in this result. These arguments have been substantiated both by instanton liquid<sup>21,22</sup> and lattice QCD simulations<sup>23,24,25,26,27,28,29,30,31</sup>.

Because of the Banks-Casher relation,  $\Sigma = \pi\rho(0)/V$ , the eigenvalues near zero are spaced as  $1/\rho(0) = \pi/\Sigma V$ . In order to study the approach to the thermodynamic limit it is natural to introduce the microscopic limit in which  $u = \lambda V \Sigma$  is kept fixed for  $V \rightarrow \infty$  and the microscopic spectral density<sup>10</sup>

$$\rho_S(u) = \lim_{V \rightarrow \infty} \frac{1}{V\Sigma} \langle \rho(\frac{u}{V\Sigma}) \rangle. \quad (1)$$

Our claim is that for  $u \ll n_c$  the microscopic spectral density is given by chRMT. Indeed, the chRMT result for (1) can be derived from pqChPT<sup>9</sup>.

The chRMT partition function is introduced in section 2. Its domain of validity is discussed in section 3 and universality arguments are presented in section 4. Lattice results are shown in section 5. Before concluding we finish with applications of chRMT to QCD at nonzero chemical potential (section 6).

## 2 CHIRAL RANDOM MATRIX THEORY

In this section we will introduce an instanton liquid<sup>32,33</sup> inspired chiral RMT with the global symmetries of the QCD partition function but otherwise Gaussian random matrix elements. For  $N_f$  flavors in the sector with topological charge  $\nu$  such chRMT is defined by<sup>10,34</sup>

$$Z_{N_f, \nu}^\beta(m_1, \dots, m_{N_f}) = \int DW \prod_{f=1}^{N_f} \det(\mathcal{D} + m_f) e^{-\frac{N\Sigma^2\beta}{4} \text{Tr} W^\dagger W}, \quad (2)$$

where

$$\mathcal{D} = \begin{pmatrix} 0 & iW \\ iW^\dagger & 0 \end{pmatrix}, \quad (3)$$

and  $W$  is a  $n \times m$  matrix with  $\nu = |n - m|$  and  $N = n + m$ . The matrix elements of  $W$  are either real ( $\beta = 1$ , chiral Gaussian Orthogonal Ensemble (chGOE)), complex ( $\beta = 2$ , chiral Gaussian Unitary Ensemble (chGUE)), or quaternion real ( $\beta = 4$ , chiral Gaussian Symplectic Ensemble (chGSE)). As is the case in QCD, we assume that  $\nu$  does not exceed  $\sqrt{N}$ , so that, to a good approximation,  $n = N/2$ . The value of the Dyson index  $\beta$  is determined by the anti-unitary symmetries of the Dirac operator. If there are no anti-unitary symmetries the value of  $\beta = 2$ . If the square of the anti-unitary symmetry operator is  $\mathbf{1}$  we have  $\beta = 1$  and if its square is  $-\mathbf{1}$  we have  $\beta = 4$ . Together with the

Dyson ensembles, the GOE, the GUE and the GSE, the chiral ensembles can be classified in terms symmetric spaces<sup>35</sup>.

In this model chiral symmetry is broken spontaneously with chiral condensate given by  $\Sigma = \lim_{N \rightarrow \infty} \pi \rho(0)/N$ , where  $N$  is interpreted as the (dimensionless) volume of space time. For complex matrix elements ( $\beta = 2$ ), which is appropriate for QCD with three or more colors and fundamental fermions, the symmetry breaking pattern is<sup>36</sup>  $SU(N_f) \times SU(N_f)/SU(N_f)$ . The average spectral density that can be derived from (2) has the familiar semi-circular shape. The microscopic spectral density for the chGUE is given by<sup>37,34</sup>

$$\rho_S(z) = \frac{z}{2} (J_a^2(z) - J_{a+1}(z)J_{a-1}(z)), \quad (4)$$

where  $a = N_f + |\nu|$ . The spectral correlations in the bulk of the spectrum are given by the invariant random matrix ensembles<sup>38,39</sup>.

### 3 DOMAIN OF VALIDITY OF chRMT

The domain of validity is best discussed within the context of partially quenched Chiral Perturbation Theory (pqChPT). This is an effective field theory for the low-energy limit of a QCD like theory that in addition to  $N_f$  sea quarks contains valence quarks and their superpartners. It allows us to calculate the valence quark mass dependence of the chiral condensate defined as

$$\Sigma_v(m_v) = \frac{1}{V} \int d\lambda \langle \rho(\lambda) \rangle \frac{2m_v}{\lambda^2 + m_v^2}. \quad (5)$$

The spectral density follows from the discontinuity of  $\Sigma_v(m_v)$ ,

$$\frac{2\pi}{V} \langle \rho(\lambda) \rangle = \lim_{\epsilon \rightarrow 0} \Sigma(i\lambda + \epsilon) - \Sigma(i\lambda - \epsilon) = \frac{2\pi}{V} \sum_k \langle \delta(\lambda + \lambda_k) \rangle, \quad (6)$$

where the average  $\langle \dots \rangle$  is with respect to the distribution of the eigenvalues. Similarly, the two-point spectral correlation function follows from the double discontinuity of the scalar susceptibility.

In both cases we can identify an important scale where the inverse mass of the Goldstone modes corresponding to the valence quark is equal to the size of the box. Using the relation  $M = (m + m')\Sigma/F^2$ , where  $F$  is the pion decay constant, we find from  $ML = 1$  that in terms of  $m$  this scale is given by<sup>22,9,40</sup>

$$E_c = \frac{F^2}{\Sigma L^2}. \quad (7)$$

For  $m_v \ll E_c$  we have shown that the valence quark mass dependence is given by the chRMT. The asymptotic result for the chRMT two-point correlation function follows from the double Goldstone pole in the scalar susceptibility. The conclusion is that if pqChPT describes correctly the low energy limit of QCD we have shown that the correlations of the Dirac eigenvalues close to zero are given by chRMT.

Such picture is well-known from mesoscopic physics<sup>5</sup>. In this context  $E_c$  is defined as the inverse tunneling time of an electron through the sample and is given by  $E_c = \hbar D/L^2$ , where  $D$  is the diffusion constant. Another scale that enters in these systems is the elastic scattering time  $\tau_e$ . Based on these scales one can distinguish three different regimes<sup>11</sup> for the energy difference,  $\delta E$ , that enters in the two-point correlation function: i) the ergodic regime for  $\delta E \ll E_c$ , ii) the diffusive domain for  $E_c \ll \delta E \ll \hbar/\tau_e$  and iii) the ballistic regime for  $\delta E \gg \hbar/\tau_e$  (not discussed below). For time scales corresponding to the ergodic regime an initially localized wave packet covers all of phase space. In this domain the eigenvalue correlations are given by RMT. In the diffusive domain an initially localized wave packet explores only part of the phase space resulting in weaker correlations between the eigenvalues. For earlier applications of localization theory to the chiral phase transition we refer to<sup>41,42</sup>.

Based on these ideas we can interpret the Euclidean Dirac spectrum as the energy levels of a Hamiltonian conjugate to an additional artificial time dimension. According to the Bohigas conjecture<sup>43</sup> the eigenvalue correlations are given by RMT if and only if the corresponding classical motion is chaotic. We thus conclude that the classical time evolution of quarks in the Yang-Mills gauge fields is chaotic.

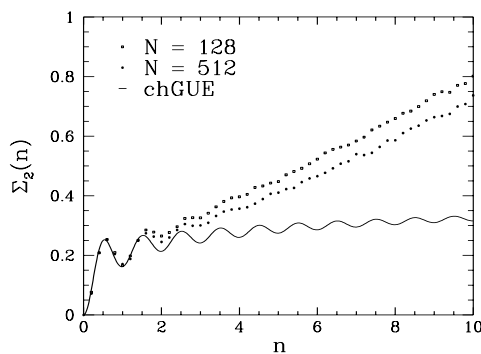


Figure 1: The number variance  $\Sigma_2(n)$  versus  $n$  measured from an interval starting at  $\lambda = 0$ . The total number of instantons is denoted by  $N$ .

These ideas can be tested by means of lattice QCD<sup>25,26</sup> and instanton liquid<sup>22</sup> simulations. In Fig. 1, we show<sup>22</sup>  $\Sigma_2(n)$ , defined as the variance of the number of levels in an interval containing  $n$  level on average, versus  $n$  for eigenvalues obtained from the Dirac operator in the background of instanton liquid gauge field configurations. The chRMT result, given by the solid curve, is reproduced up to about two level spacings. In units of the average level spacing,  $\Delta = 1/\rho(0) = \pi/\Sigma V$ , the energy  $E_c$  is given by  $n_c \equiv E_c/\Delta = F^2 L^2/\pi$ . For an instanton liquid with instanton density  $N/V = 1$  we find that  $n_c \approx 0.07\sqrt{N}$ . We conclude that chRMT appears to describe the eigenvalue correlations up to the predicted scale.

The additional two flavors in Damgaard's relation<sup>16</sup> between the microscopic spectral density and the finite volume partition function arise naturally in pqChPT<sup>9</sup>, namely one valence flavor and its supersymmetric partner.

#### 4 UNIVERSALITY IN CHIRAL RANDOM MATRIX THEORY

The aim of universality studies is to identify observables that are stable against deformations of the random matrix ensemble. Not all observables have the same degree of universality. For example, a semicircular average spectral density is found for random matrix ensembles with independently distributed matrix elements with a finite variance. However, this spectral shape does not occur in nature, and it is thus not surprising that it is only found in a rather narrow class of random matrix ensembles. What is surprising is that the *microscopic* spectral density and the *microscopic* spectral correlators are stable with respect to a much larger class of deformations. Two different types of deformations have been considered, those that maintain the unitary invariance of the partition functions and those that break the unitary invariance.

In the first class, the Gaussian probability distribution is replaced by  $P(W) \sim \exp(-N \sum_{k=1}^{\infty} a_k \text{Tr}(W^\dagger W)^k)$ . For a potential with only  $a_1$  and  $a_2$  different from zero it was shown<sup>12</sup> that the microscopic spectral density is independent of  $a_2$ . A general proof valid for arbitrary potential and all correlation functions was given by Akemann et al.<sup>13</sup>. The essence of the proof is a remarkable generalization of the identity for the Laguerre polynomials,  $\lim_{n \rightarrow \infty} L_n(x/n) = J_0(2\sqrt{x})$ , to orthogonal polynomials determined by an arbitrary potential. It was proved from the continuum limit of the recursion relation for orthogonal polynomials.

In the second class, an arbitrary fixed matrix is added to  $W$  in the Dirac operator (3). It has been shown that the microscopic spectral density and the microscopic spectral correlations remain unaffected<sup>14,15</sup> for parameter values

that completely modify the average spectral density.

Microscopic universality for deformations that affect the macroscopic spectral density implies the existence of a scale beyond which universality breaks down. It can be interpreted naturally in terms of the spreading width<sup>44</sup>.

Based on the general form of the pqChPT partition function one could argue that universality follows from its relation with chRMT. However, universality can be formulated as the stability of the effective partition function with respect to variations of the distribution of matrix elements. The stability of the saddle-point manifold was demonstrated for the Unitary ensembles<sup>45</sup>.

## 5 LATTICE QCD RESULTS

In this section we consider correlations of lattice QCD Dirac eigenvalues. For a Dirac operator with a  $U_A(1)$  symmetry the eigenvalues occur in pairs  $\pm\lambda_k$ . Therefore we have to distinguish two different regions: the region near zero virtuality and the bulk of the spectrum. The  $U_A(1)$  symmetry is absent for the Hermitean Wilson Dirac operator which includes an additional  $\gamma_5$  matrix.

The relevant class of random matrix ensembles is determined by the anti-unitary symmetries of the Dirac operator. For the  $SU(2)$  color group, the anti-unitary symmetries of the Kogut-Susskind (KS) and the Wilson Dirac operator are given by<sup>46,28</sup>,

$$[D^{KS}, \tau_2 K] = 0, \quad \text{and} \quad [\gamma_5 D^W, \gamma_5 C K \tau_2] = 0. \quad (8)$$

Because  $(\tau_2 K)^2 = -1$  and  $(\gamma_5 C K \tau_2)^2 = 1$ , we have  $\beta = 1$  for Wilson fermions and  $\beta = 4$  for KS fermions. This results in the chGUE for KS fermions and, in absence of the  $U_A(1)$  symmetry, in the GOE for Wilson fermions<sup>28</sup>. For three or more colors there are no anti-unitary symmetries and the relevant ensembles are the chGUE and GUE for KS and Wilson fermions, respectively.

The eigenvalue correlations, which are separated from the average spectral density by calculating them for the unfolded eigenvalues, are studied by means of moments of the number of levels,  $n_i$ , in an interval containing  $n$  levels on average. Below we discuss the variance,  $\Sigma_2(n)$  and the first two cumulants  $\gamma_1(n)$  and  $\gamma_2(n)$ . The moments can be obtained either by ensemble averaging or by spectral averaging. Under the assumption of spectral ergodicity, both procedures should give the same results. However, recent results<sup>26</sup> indicate that the domain of RMT correlations is the much longer for spectral averaging than for ensemble averaging. This interesting observation certainly deserves more attention.

Results obtained by spectral averaging for  $\Sigma_2(n)$ ,  $\gamma_1(n)$  and  $\gamma_2(n)$  for both KS and Wilson fermions with  $N_c = 2$  (see Fig. 2) show an impressive agreement with the RMT predictions. This agreement extends to a wide range of

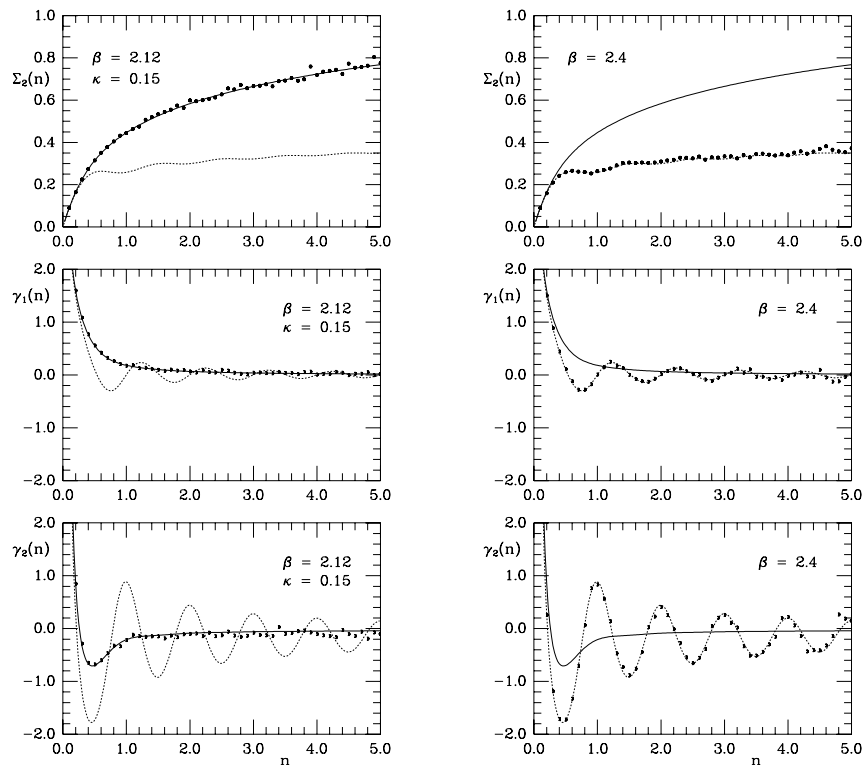


Figure 2: The number variance,  $\Sigma_2(n)$ , and the first two cumulants,  $\gamma_1(n)$  and  $\gamma_2(n)$ , as a function of  $n$ .

$\beta$  values ranging from strong coupling to weak coupling. The simulations for KS fermions were performed<sup>47</sup> for 4 dynamical flavors with  $ma = 0.05$  on a  $12^4$  lattice. The simulations for Wilson fermions were done for two dynamical flavors on a  $8^3 \times 12$  lattice. Recently, impressive results were obtained for the nearest neighbor spacing distribution of  $N_c = 3$  staggered Dirac spectra<sup>30</sup>.

Spectral ergodicity cannot be exploited in the study of the microscopic spectral density. In order to gather sufficient statistics, a large number of independent spectra is required. One way to proceed is to use instanton-liquid configurations which can be generated cheaply. In this case we find<sup>21</sup> that the microscopic spectral density is given by the chGOE and the chGUE for  $N_c = 2$  and  $N_c = 3$ , respectively. Recently, this analysis was performed for lattice QCD Dirac eigenvalues<sup>23</sup>. Results for 1416 quenched  $SU(2)$  Kogut-Susskind Dirac

spectra on a  $10^4$  lattice are shown in Fig. 3. We show both the distribution of the smallest eigenvalue (left) and the microscopic spectral density (right). The results for the chGSE are represented by the dashed curves. We emphasize that

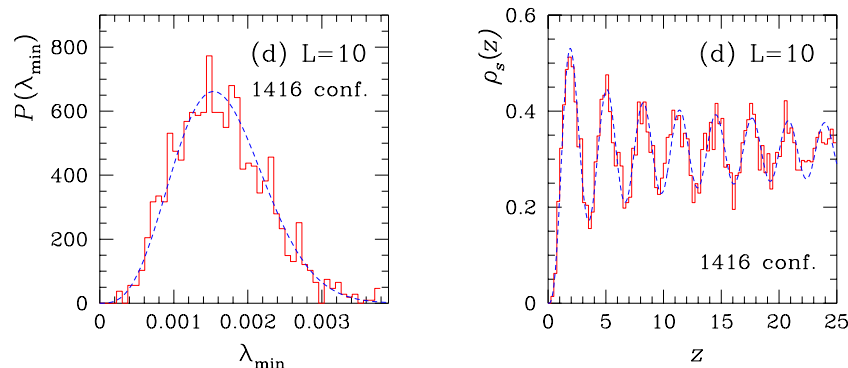


Figure 3: The distribution of the smallest eigenvalue (left) and the microscopic spectral density (right) for two colors and  $\beta = 2.0$ .

the theoretical curves have been obtained without any fitting of parameters. The input parameter, the chiral condensate, is derived from the same lattice calculations. The above simulations were performed at a relatively strong coupling of  $\beta = 2$ , but agreement with the chGSE predictions was also found for  $\beta = 2.2$  and for  $\beta = 2.5$  on a  $16^4$  lattice<sup>23</sup>.

In the case of two fundamental colors the continuum theory and Wilson fermions are in the same universality class. It is an interesting question of how spectral correlations of KS fermions evolve in the approach to the continuum limit. Certainly, the Kramers degeneracy of the eigenvalues remains. However, since Kogut-Susskind fermions represent 4 degenerate flavors in the continuum limit, the Dirac eigenvalues should obtain an additional two-fold degeneracy. We are looking forward to more work in this direction.

## 6 APPLICATIONS OF chRMT AT $\mu \neq 0$

In the continuum formulation of QCD the chemical potential enters in the QCD partition function by the addition of the term  $\mu\gamma_0$  to the anti-Hermitian Dirac operator, i.e.  $\mathcal{D} \rightarrow \mathcal{D} + \mu\gamma_0$ . In a suitable chiral basis in which the matrix elements of  $\langle \phi_R^k | \gamma_0 | \phi_L^k \rangle = \delta_{kl}$ , the modification in the random matrix



partition function (2) corresponds to replacing the Dirac matrix  $\mathcal{D}$  by

$$\mathcal{D} = \begin{pmatrix} 0 & iW + \mu \\ iW^\dagger + \mu & 0 \end{pmatrix}. \quad (9)$$

The term  $\mu\gamma_0$  has the same anti-unitary symmetries as  $\gamma_0\partial_0$  and therefore does not alter the corresponding classification of the Dirac operators.

As is the case in QCD<sup>48</sup>, a nonzero chemical potential violates the anti-Hermiticity of the Dirac operator and its eigenvalues are scattered in the complex plane. One important result obtained from the chRMT at  $\mu \neq 0$  is that the quenched approximation is the limit  $N_f \rightarrow 0$  of the partition function with the determinant replaced by its absolute value<sup>49</sup>. By replacing  $\mu \rightarrow \mu + iT$  one obtains a Landau-Ginzburg functional for the order parameter<sup>50</sup>. A similar Landau-Ginzburg functional has been derived from the Nambu model<sup>51</sup>. For  $\mu = 0$  this model undergoes a second order phase transition<sup>52,53,54</sup>. At  $T = 0$  we find a first order phase transition<sup>49</sup>. A tricritical point is found for at  $m = 0$ ,  $\mu \neq 0$  and  $T \neq 0$ . For more discussion of this model we refer to the literature<sup>55</sup>.

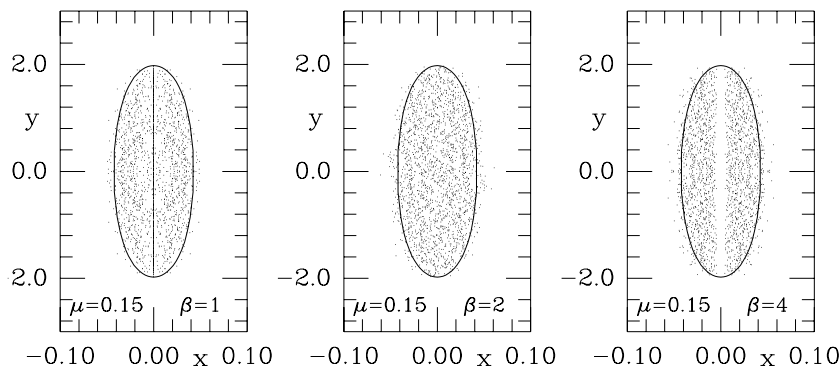


Figure 4: Scatter plot of the real ( $x$ ), and the imaginary parts ( $y$ ) of the eigenvalues of the random matrix Dirac operator at  $\mu \neq 0$ .

We close this lecture with identifying possible universal behavior at  $\mu \neq 0$ . Quenched numerical simulations have been performed for all three classes of  $\beta$ . A cut along the imaginary axis below cloud of eigenvalues was found in instanton liquid simulations<sup>56</sup> for  $N_c = 2$  at  $\mu \neq 0$  ( $\beta = 1$ ). In lattice QCD simulations with staggered fermions<sup>57</sup> for  $N_c = 2$  ( $\beta = 4$ ) a depletion of eigenvalues along the imaginary axis was observed whereas for  $N_c = 3$  ( $\beta = 2$ ), the eigenvalue distribution did not show any pronounced features.

In the quenched approximation, the spectral properties of the random matrix ensemble (9) can be studied numerically by simply diagonalizing a set of matrices with probability distribution (2). In Fig. 4 we show results<sup>58</sup> for the eigenvalues of a few  $100 \times 100$  matrices for  $\mu = 0.15$  (dots) of the quenched random matrix ensemble (9). The solid curve represents the analytical result for the boundary of the domain of eigenvalues<sup>49,58</sup>. We observe the accumulation and depletion that was found in the previously mentioned simulations. This depletion can be understood as follows. For  $\mu = 0$  all eigenvalues are doubly degenerate. This degeneracy is broken at  $\mu \neq 0$  which produces the observed repulsion of the eigenvalues.

The number of purely imaginary eigenvalues for  $\beta = 1$  appears to scale as  $\sqrt{N}$  which has been understood analytically for ensembles without a chiral structure<sup>59</sup>. Obviously, more work has to be done in order to arrive at a complete characterization of universal features<sup>60</sup> of nonhermitean matrices.

## 7 CONCLUSIONS

We have presented both analytical and numerical arguments showing that the correlation of the QCD Dirac eigenvalues below a scale of  $\sim \Lambda_{QCD}/L^2$  are given by chRMT. We conclude that if partially quenched chiral perturbation theory is the correct description of the low energy limit of QCD, we have shown that below the Thouless energy, the eigenvalue correlations are given by chRMT. Our confidence in these arguments has been strengthened by universality studies. Universal features in Dirac spectra at nonzero chemical potential have been identified.

## Acknowledgments

This work was partially supported by the US DOE grant DE-FG-88ER40388. The TPI at Minneapolis is thanked for its hospitality. Useful discussions with B. Altshuler, P. Damgaard, T. Guhr, Y. Fyodorov, B. Shklovskii, A. Smilga, H. Weidenmüller and T. Wettig are acknowledged. D. Toublan is thanked for a critical reading of the manuscript. Finally, I thank my collaborators on whose work this review is based.

## References

1. T. Banks and A. Casher, Nucl. Phys. **B169** (1980) 103.
2. J. Gasser and H. Leutwyler, Phys. Lett. **188B**(1987) 477.
3. H. Leutwyler and A. Smilga, Phys. Rev. **D46** (1992) 5607.
4. J. Verbaarschot, hep-th/9710114.

5. T. Guhr, A. Müller-Groeling and H.A. Weidenmüller, Phys. Rep. **299** (1998) 189.
6. C. Bernard and M. Golterman, Phys. Rev. D **49** (1994) 486; C. Bernard and M. Golterman, hep-lat/9311070.
7. A. Morel, J. Physique **48** (1987) 1111.
8. C. Vafa and E. Witten, Nucl. Phys. **B234** (1984) 173.
9. J. Osborn, D. Toublan and J. Verbaarschot, hep-th/9806110.
10. E. Shuryak and J. Verbaarschot, Nucl. Phys. **A560** (1993) 306.
11. B. Altshuler, I. Zharekeshev, S. Kotochigova and B. Shklovskii, Zh. Eksp. Teor. Fiz. **94** (1988) 343.
12. E. Brézin, S. Hikami and A. Zee, Nucl. Phys. **B464** (1996) 411.
13. G. Akemann, P. Damgaard, U. Magnea and S. Nishigaki, Nucl. Phys. **B487**[FS] (1997) 721; hep-th/9712006.
14. T. Guhr and T. Wettig, Nucl. Phys. **B506** (1997) 589.
15. A. Jackson, M. Sener and J. Verbaarschot, Nucl. Phys. **B479** (1996) 707; Nucl. Phys. **B506** (1997) 612.
16. P. Damgaard, Phys. Lett. **B424** (1998) 322; G. Akemann and P. Damgaard, hep-th/9802174; hep-th/9801133.
17. K. Splittorff and A. Jackson, hep-lat/9805018.
18. S. Nishigaki, P. Damgaard and T. Wettig, hep-th/9803007.
19. M. Sener and J. Verbaarschot, Phys. Rev. Lett. (in press), hep-th/9801042; H. Widom, solv-int/9804005.
20. E. Brézin and S. Hikami, cond-mat/9804023.
21. J. Verbaarschot, Nucl. Phys. **B427** (1994) 434.
22. J. Osborn and J. Verbaarschot, Phys. Rev. Lett. (in press) (1998); Nucl. Phys. **B** (in press) (1998), hep-ph/9803419.
23. M. Berbenni-Bitsch, S. Meyer, A. Schäfer, J. Verbaarschot and T. Wettig, Phys. Rev. Lett. **80** (1998) 1146.
24. J.Z. Ma, T. Guhr and T. Wettig, Eur. Phys. J. **A2** (1998) 87.
25. M. Berbenni-Bitsch, *et al.*, hep-ph/9804439.
26. T. Guhr, J.Z. Ma, S. Meyer and T. Wilke, hep-lat/9806003.
27. M. Berbenni-Bitsch, S. Meyer and T. Wettig, hep-lat/9804030.
28. M. Halasz and J. Verbaarschot, Phys. Rev. Lett. **74** (1995) 3920.
29. M. Halasz, T. Kalkreuter and J. Verbaarschot, Nucl. Phys. Proc. Suppl. **53** (1997) 266.
30. R. Pullirsch, K. Rabitsch, T. Wettig and H. Markum, hep-ph/9803285.
31. V. Azcoiti, V. Laliena and X.-Q. Luo, Phys. Lett. **B354** (1995) 111.
32. T. Schäfer and E. Shuryak, Rev. Mod. Phys. **70** (1998) 323.
33. D. Diakonov and V. Petrov, Nucl. Phys. **B272** (1986) 457.
34. J. Verbaarschot, Phys. Rev. Lett. **72** (1994) 2531; Phys. Lett. **B329**

- (1994) 351.
35. M. Zirnbauer, J. Math. Phys. **37** (1996) 4986; F.J. Dyson, Comm. Math. Phys. **19** (1970) 235.
  36. A. Smilga and J. Verbaarschot, Phys. Rev. **D51** (1995) 829.
  37. J. Verbaarschot and I. Zahed, Phys. Rev. Lett. **70** (1993) 3852.
  38. D. Fox and P. Kahn, Phys. Rev. **134** (1964) B1152; (1965) 228.
  39. T. Nagao and M. Wadati, J. Phys. Soc. Japan **60** (1991) 2998, 3298; **61** (1992) 78, 1910.
  40. R. Janik, G. Papp, M. Nowak and I. Zahed, hep-ph/9803289.
  41. E. Shuryak, Nucl. Phys. **B302** (1988) 599; D. Diakonov, hep-ph/9602375; J. Stern, hep-ph/9801282.
  42. A. Smilga, Phys. Rep. **291** (1997) 1.
  43. O. Bohigas, M. Giannoni and C. Schmit, Phys. Rev. Lett. **52** (1984) 1.
  44. H.A. Weidenmüller, Nucl. Phys. **A 518** (1990) 1.
  45. G. Hackenbroich and H. Weidenmüller, Phys. Rev. Lett. **74** (1995) 4118.
  46. S. Hands and M. Teper, Nucl. Phys. **B347** (1990) 819.
  47. T. Kalkreuter, Phys. Lett. **B276** (1992) 485; Phys. Rev. **D48** (1993) 1; Comp. Phys. Comm. **95** (1996) 1.
  48. I. Barbour, N. Behihil, E. Dagotto, F. Karsch, A. Moreo, M. Stone and H. Wyld, Nucl. Phys. **B275** (1986) 296; M.-P. Lombardo, J. Kogut and D. Sinclair, Phys. Rev. **D54** (1996) 2303.
  49. M. Stephanov, Phys. Rev. Lett. **76** (1996) 4472.
  50. M. Halasz, A. Jackson, R. Shrock, M. Stephanov and J. Verbaarschot, hep-ph/9804290.
  51. J. Berges and K. Rajagopal, hep-ph/9804233.
  52. A. Jackson and J. Verbaarschot, Phys. Rev. **D53** (1996) 7223.
  53. T. Wettig, A. Schäfer and H. Weidenmüller, Phys. Lett. **B367** (1996) 28.
  54. M. Stephanov, Phys. Lett. **B275** (1996) 249; Nucl. Phys. Proc. Suppl. **53** (1997) 469.
  55. J. Feinberg and A. Zee, Nucl. Phys. **B504** (1997) 579; Nucl. Phys. **B501** (1997) 643; R. Janik, M. Nowak, G. Papp, and I. Zahed, Acta Phys. Polon. B **28** (1997) 2949; M. Halasz, A. Jackson and J. Verbaarschot, Phys. Lett. **B395** (1997) 293; Phys. Rev. **D56** (1997) 5140.
  56. Th. Schäfer, Phys. Rev. **D57** (1998) 3950.
  57. C. Baillie, K. Bowler, P. Gibbs, I. Barbour and M. Rafique, Phys. Lett. **197B**, 195 (1987).
  58. M. Halasz, J. Osborn and J. Verbaarschot, Phys. Rev. **D56** (1997) 7059.
  59. Y. Fyodorov, B. Khoruzhenko and H. Sommers, Phys. Lett. **A 226**

- (1197) 46 ; K. Efetov, Phys. Rev. Lett. **79** (1997) 491; Phys. Rev. **B**  
**56** (1997) 9630.
60. Y. Fyodorov, B. Khoruzhenko and H. Sommers, Phys. Rev. Lett. **79**  
(1997) 557; Y. Fyodorov, M. Titov and H. Sommers, cond-mat/9802306.